INTRODUCTION

Introduction

A) Introduction to the chemistry of curcumin

1. introduction and scope

INDIA has a rich history of using plants for medicinal purposes. Turmeric (*Curcuma longa* L.) is a medicinal plant extensively used in Ayurveda, Unani and Siddha medicine as home remedy for various diseases.[1,2] *C. longa* L., botanically related to ginger (Zingiberaceae family), is a perennial plant having a short stem with large oblong leaves and bears ovate, pyriform or oblong rhizomes, which are often branched and brownish-yellow in colour. Turmeric is used as a food additive (spice), preservative and colouring agent in Asian countries, including China and South East Asia. It is also considered as auspicious and is a part of religious rituals. In old Hindu medicine, it is extensively used for the treatment of sprains and swelling caused by injury.[1] In recent times, traditional Indian medicine uses turmeric powder for the treatment of biliary disorders, anorexia, coryza, cough, diabetic wounds, hepatic disorders, rheumatism and sinusitis.[3]

In China, *C. longa* is used for diseases associated with abdominal pains.[4] The colouring principle of turmeric is the main component of this plant and is responsible for the anti-inflammatory property. Turmeric was described as *C. longa* by Linnaeus and its taxonomic position is as follows:

Class Liliopsida

Subclass Commelinids

Order Zingiberales

Family Zingiberaceae

Genus *Curcuma*

Species *Curcuma longa*

The wild turmeric is called *C. aromatica* and the domestic species is called *C. longa*.

Chemical composition of turmeric

Turmeric contains protein (6.3%), fat (5.1%), minerals (3.5%), carbohydrates (69.4%) and moisture (13.1%). The essential oil (5.8%) obtained by steam distillation of rhizomes has α-phellandrene (1%), sabinene (0.6%), cineol (1%), Borneo (0.5%), zingiberene (25%) and sesquiterpines (53%).[5] Curcumin (diferuloylmethane) (3–4%) is responsible for the yellow colour, and comprises curcumin **I** (94%), curcumin **II** (6%) and curcumin **III** (0.3%).[6] Demethoxy and bisdemethoxy derivatives of curcumin have also been isolated,[7] Curcumin was first isolated.[8] in 1815 and its chemical structure was determined by Roughley and Whiting.[9] in 1973. It has a melting point at 176–177°C; forms a reddish-brown salt with alkali and is soluble in ethanol, alkali, ketone, acetic acid and chloroform.

2. Synthesis of curcuminoide derivatives

The first trial for the preparation of curcumin derivative **(1)** was reported in 1913.[10] Treatment of cinnamic acid derivatives with acetyl chloride afforded the corresponding cinnamoyl chloride **(2)**. The reaction of **(2)** with diethyl malonate gives the corresponding diester **(3)** which gave the ester **(4)** after hydrolysis and decarboxylation **(Scheme 1)**.

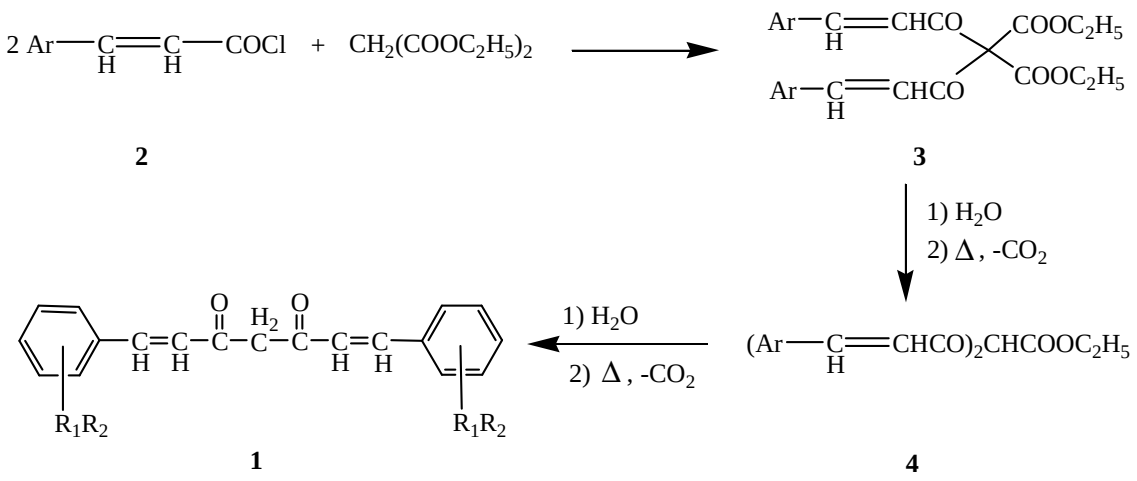

Scheme 1

The ester **(4)** was then subjected once again to hydrolysis and decarboxylation process to give finally the curcumin derivative **(1)**.

On the other hand, treatment of the cinnamoyl chloride **(2)** with ethyl acetoacetate afforded the *β*-keto ester **(5)**. Compound **(5)** upon hydrolysis and decarboxylation gives the 1,3- diketone **(6)**. While treatment of **(6)** with substituated benzaldehyde in basic medium afforded the corresponding curcumin derivatives **(1) (Scheme 2)**.

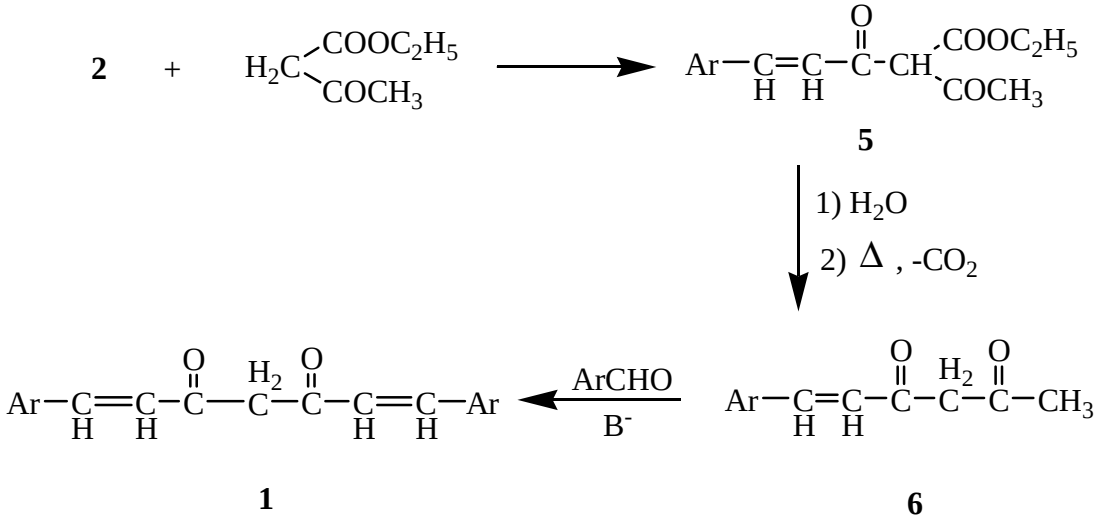

Scheme 2

A convenient reaction leading to the synthesis of curcumin **(1)** from acetylacetone has been reported by pabon in 1964.[11] curcumin **(1)** was prepared in 80% yield from vaniline **(8)** and acetylacetone **(7)**- B_2O_3 in the

presence of tri-sec-butylborate **(9)** and $BuNH_2$. The reaction was repeated in ethyl acetate at room temperature: eight- compounds related to **(1)** were also synthesized **(Scheme 3)**.

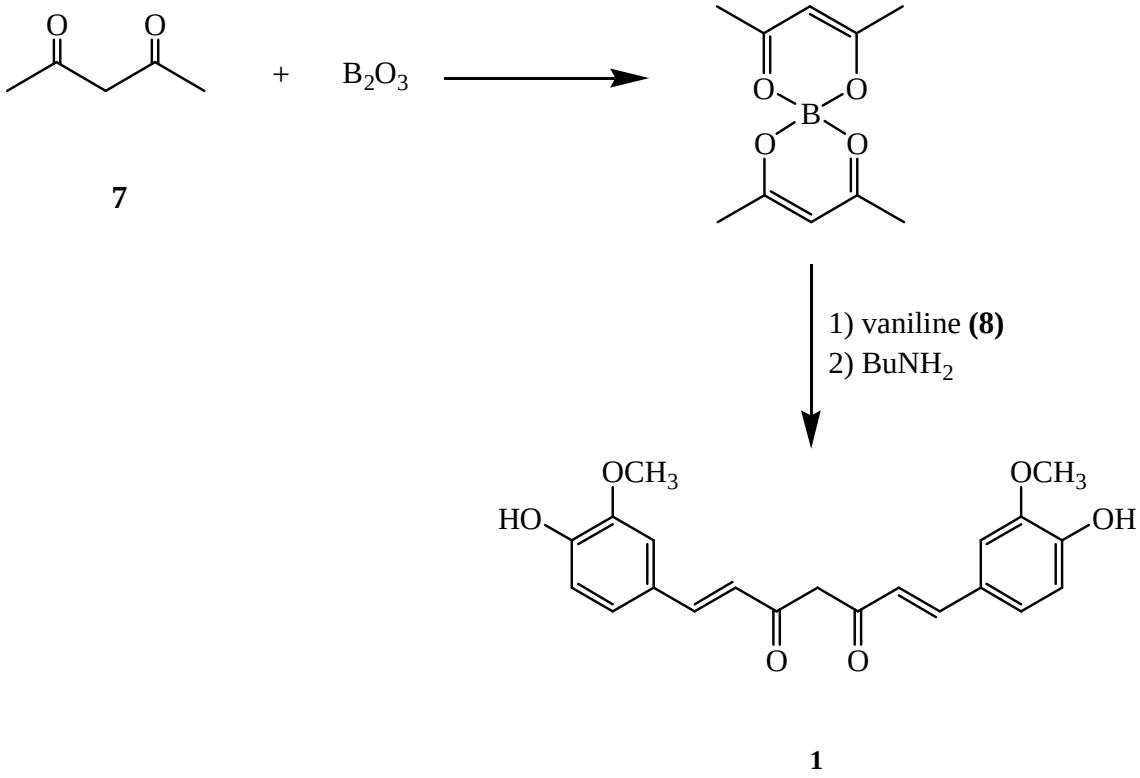

7 **1**

Scheme 3

It has also been reported In *german pat* .[12] that, symmetrical 1,3-diketones are obtained generally with good yield from reaction of vinyl acetate **(10)** (or formate, butyrate, hexanoate, palmitate) with aliphatic, aromatic, arylaliphatic or cycloaliphatic acid chloride in presence of $AlCl_3$ or $FeCl_3$ in tetrachloroethylene or carbon disulphide and hydrolysis of the compound formed. Curcumin **(1)** (diferuloyl methane), is obtained from reaction of carbomethoxy feruloyl chloride **(11)** in CS_2 mixed with $AlCl_3$ and compound **(10)**.

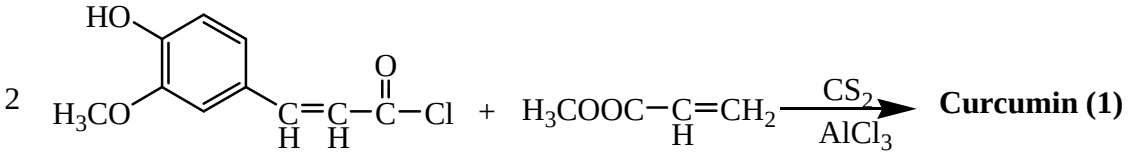

11 **10**

Similar to the above reaction of pabon, Graf Erich,[13] prepared curcumin **(1)** in a similar manner by converting vanillin **(8)** with acetylacetone **(7)** in the presence of boron anhydride and diallyl amine or its acetate in the melt at 120-30^{o} and subsequently acidfying the mixture with acetic acid.

Peter J.Roughley,[9] reported a convenient biosynthesis for curcumin **(1)**. Curcumin the yellow pigment of curcuma longa (turmeric) and other curcuma spp., has attracted few modern studies, although isolated as early as 1815.[8] Its structure was elucidated in 1910 by Lampe,[14] and Co. Workers, who latter completed a synthesis.[10] Renewed interest has been evoked by the recent discovery of relative sharing the 1,7-diaryl skeleton. These include 4-hydroxy-cinnamoyl-(4-hydroxy-3-methoxy cinnamoyl)methane **(1)** and bis-(4-hydroxcinnamoyl)methane **(1a)**,[15] (both from curcuma spp.).

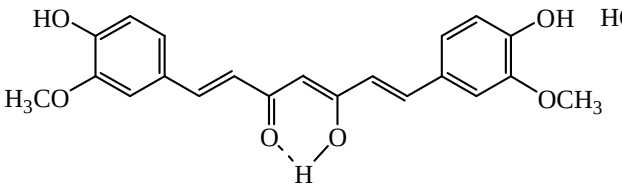

1

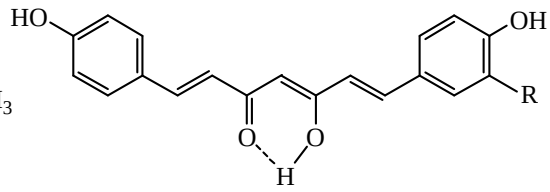

1, R= OMe
1a, R= H

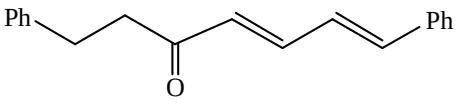

12

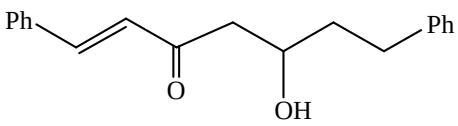

13

The simpler diaryl heptanoids **(1, 1a, 12, 13)** show a pattren of 3 (5) oxygenation (in the heptan chain), and 1,2 (6,7) unsaturation is common. This pattren has provoked the very reasonable suggestion that the biosynthesis of curcumin involves two cinnamate units which are coupled to a ceuteral carbon provided by malonate **(scheme 4)**, and it was in the

expectation of supporting the out line of this scheme that, following structural work in this area.[16]

Curcumin was chosen for biosynthetic study since it occurs in the rhizomes of the tropical perennial curcuma longa, which are suitable for in vivo experiments, unlike most other sources of diarylheptanoids.

The curcuminoids **(1,1a)** were extracted from rhizomes by benzene extraction; purification by PLC being satisfactory. NMR spectra indicate that all the diketones **(1-3)** exist in the enolic forms, interchange between enols is rapid. The enolic protons **(1,1a)** can be observed in the NMR spectrum in acetone solution at -90^{o}C, although they are not apparent at room temperature.

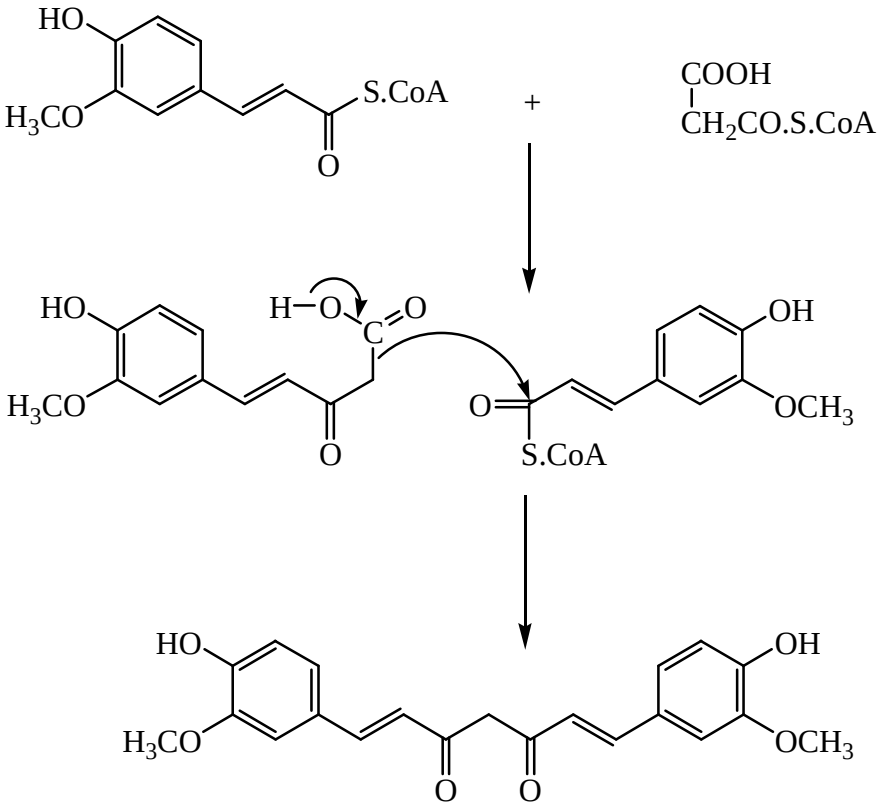

1

Scheme 4

If **scheme 4** operates for the biosynthesis of curcumin, it would be predicted the [2-C^{14}] acetate or malonate precursor would provide the

central carbon (C-1). The polyketide biosynthesis, suggests a possible alternative route **(scheme 5)** for curcumin formation. This could involve a cinnamate starter, extended by five acetate (malonate) units. Cyclization of the chain gives the second aromatic ring (reduction before cyclization removes the 6'- and (*O*'-hydroxy- functions), and biosynthesis would be completed by hydroxylation at C-7'.

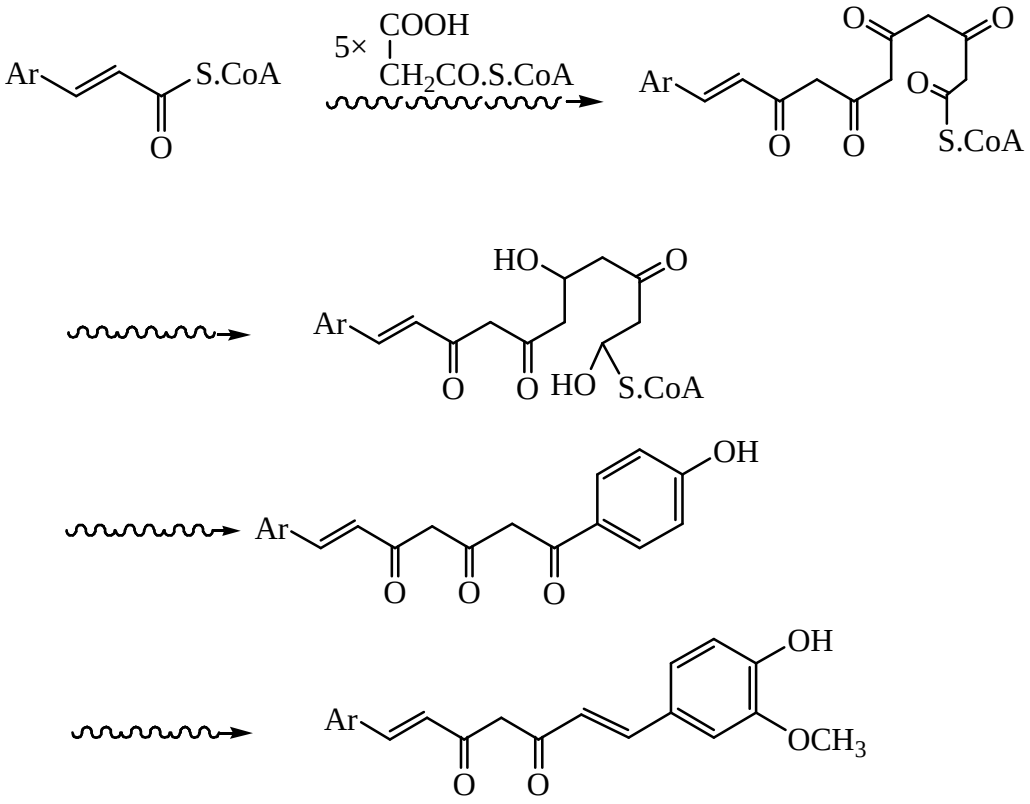

Scheme 5

The labeling expts. did not permit differentiation between formation of **(1)** (R= R'= OMe) by condensation of **(2)** cinnamate units and **(1)** malonate unit or by chain extension of cinnamate by **(5)** acetate (or malonate) units followed by cyclization and reduction.

For many centuries the roots of *curcuma longa* have been used as a yellow dye for foods and spices.[17] Different yellow pigments have been isolated from the roots.[18] and curcumin was found to be the main

compound.[19] Curcuminoids,[20] (25 compounds) were prepared by condensing different substituted 2,4-pentanediones and aromatic aldehyde (not benzaldehyde). In order to avoid knoevenagel condensation at C-3 of 2,4-pentanedione, it is necessary to protect C-3 by a boron complex, which is suggested to have the structure **(14)**.[11] Then the condensation will occure only on the terminal methyl group. In the case of 3-substituated 2,4-pentanediones it should be necessary to use a boron complex. After condensation of aldehydes with boron complex, a dark red mixture is obtained, which is easily hydrolyzed by dilute hydrochloric acid.

Some curcuminoids containing hydroxy groups in the aromatic moiety have been acylated.

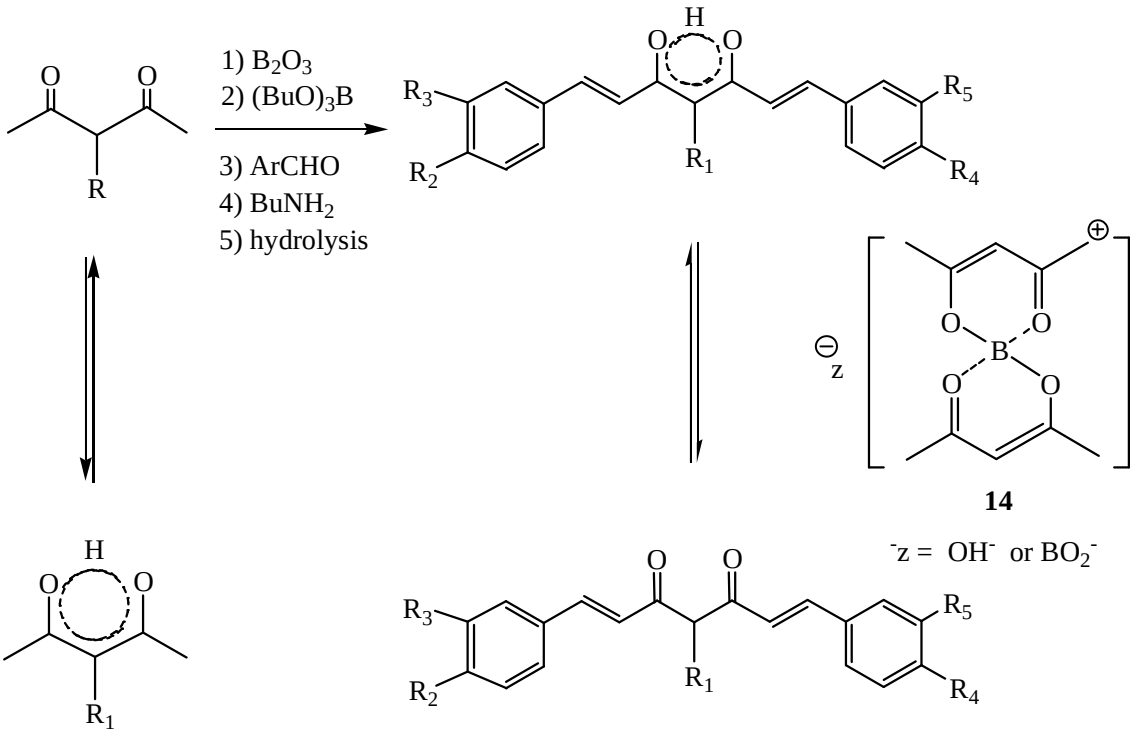

Scheme 6

Alkylation,[20] of curcumin by methyl iodide or dimethyl sulfate has shown that *O*-alkylation takes place at the phenolic oxygen and C-alkylation at C-4. No alkylation takes place at the oxygen of the enol form.

1 $\xrightarrow[2)C_6H_5CH_2Br]{1)NaOH + Bu_4NHSO_4}$ 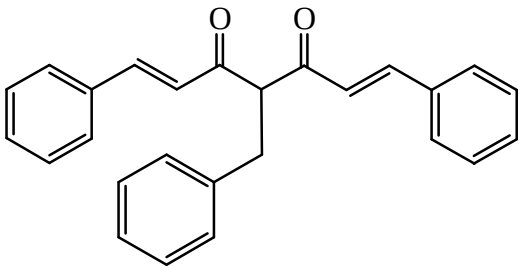

15

However, alkylations of 1,3-diketones as tetrabutyl ammonium salts give both O- and C-alkylation.[21] Reaction of the tetrabutyl ammonium salt of 5-hydroxy-1,7-diphenyl-1,4,6-heptatrien-3-one with benzyl bromide gave only C-alkylation and the isolated compound **(15)** exists only in the di keto form.

Kuroyanagi *et. al,*[18] isolated curcumin from zedoary, the rhizome of *curcuma zedoaria*. Compounds **(1-1d)** were isolated by repeated silica gel chromatography,[22] with the guidance of their yellow colour, from the EtOAc - soluble part of the MeOH extract from dry rhizomes of C. domestica

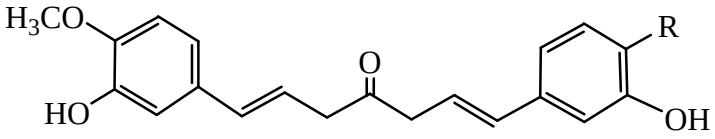

1, R= OCH_3
1b, R= H

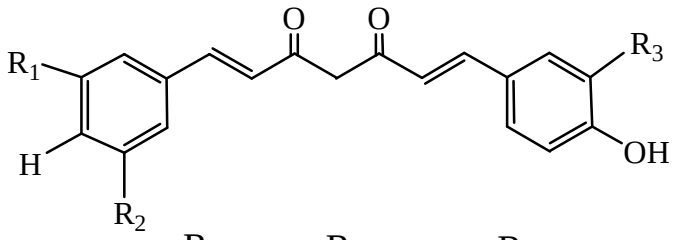

	R_1	R_2	R_3
1	OCH_3	H	OCH_3
1a	OCH_3	H	H
1c	H	H	H
1d	OCH_3	OCH_3	OCH_3

Compounds **(1-1d)** were identified as curcumin **(1)**, demethoxycurcumin **(1a)**, bisdemethoxycurcumin **(1c)** and 5'-

methoxycurcumin **(1d)**, respectively, by spectroscopic methods and direct comparisons with the authentic samples previously isolated as potent anti-oxidants from curcuma xauthorrhiza.[23]

In a similar manner to the methods of Pabon and uffe pedersen,[20] AN Nurfina,[24] extended the study of such reaction. The main feature in this process (as shown bellow) are:

a) the protection of the active methylene group by reacting the acetylacetone with boric anhydride in order to produce the acetylacetone-boric anhydride complex **(14)**;

b) the less reactive methyl terminals of this complex will react with aldehyde group of vaniline in order to give curcumin in the form of the complex with boron **(16)**;

c) the complex is then decomposed by using either dilute acids or bases; dilute acid is preferable, since curcumin itself is unstable under alkaline conditions. **(Scheme 7)**.

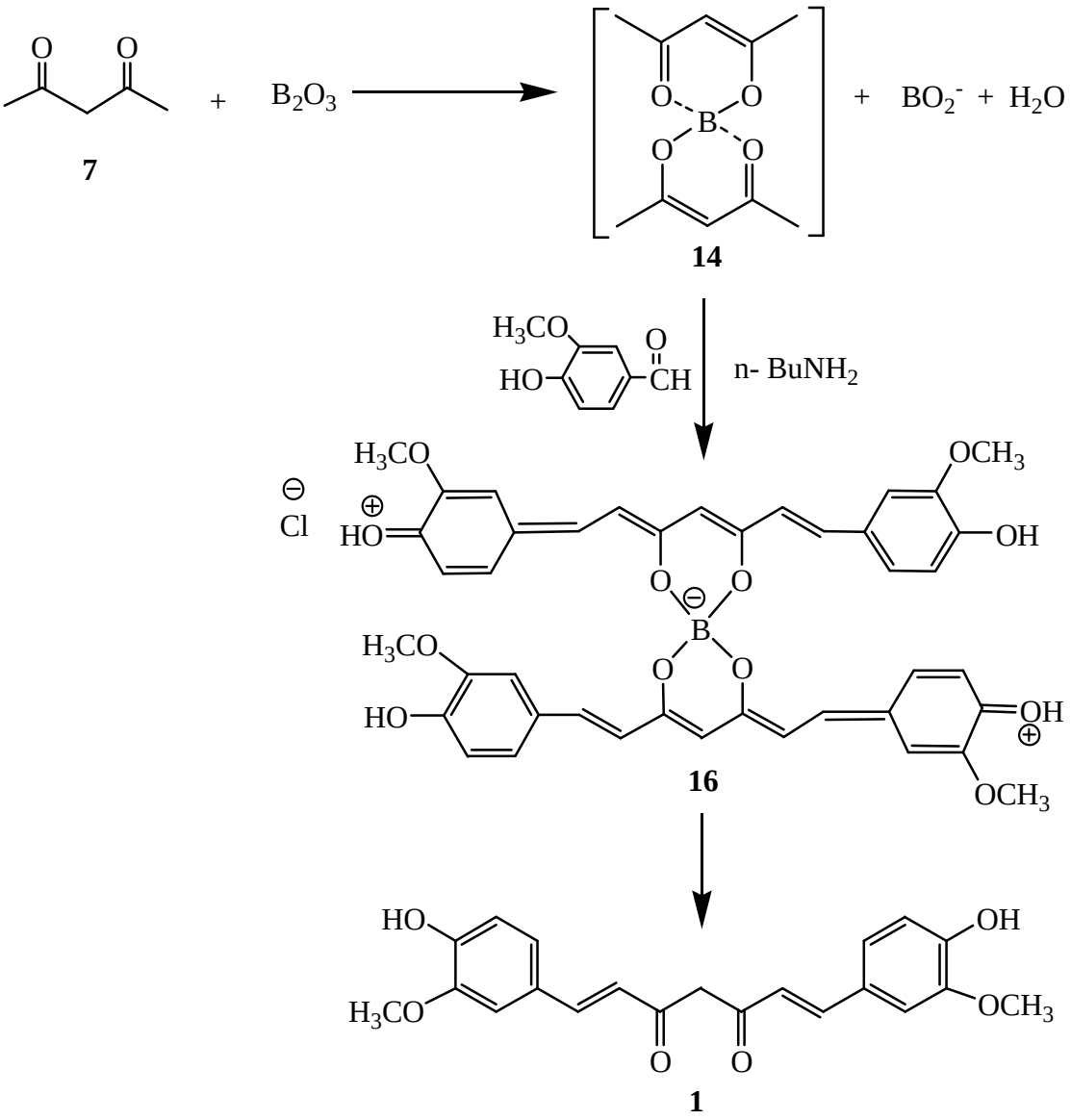

Scheme 7

Similar to the above reaction, Somepalli V. M. *et al.*[25] extended the study of reactions of acetylacetone with substituated benzaldehyde.

The curcumin analogs **(1-1b)** were synthesized by slight modification of Pabon method.[11] The main steps in this scheme are the protection of active methylene group by reacting with acetylacetone in the presence of boric oxide in order to get acetylacetone-boric oxide complex **(14)** and reacting less reactive methyls with the aldehyde group using 1,2,3,4-tetrahydroquinoline as catalyst **(scheme 4)**. Finally, the boron complex of

the product was decomposed using aq. acetic acid to get the desired curcumin analogs **(Scheme 8)**.

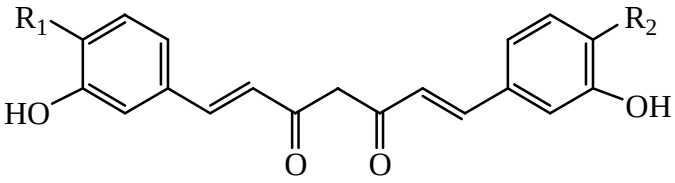

1. Curcumin; $R_1 = R_2 = OCH_3$
1a. Demethoxycurcumin; $R_1 = OCH_3$, $R_2 = H$
1b. Bisdemethoxycurcumin; $R_1 = R_2 = H$

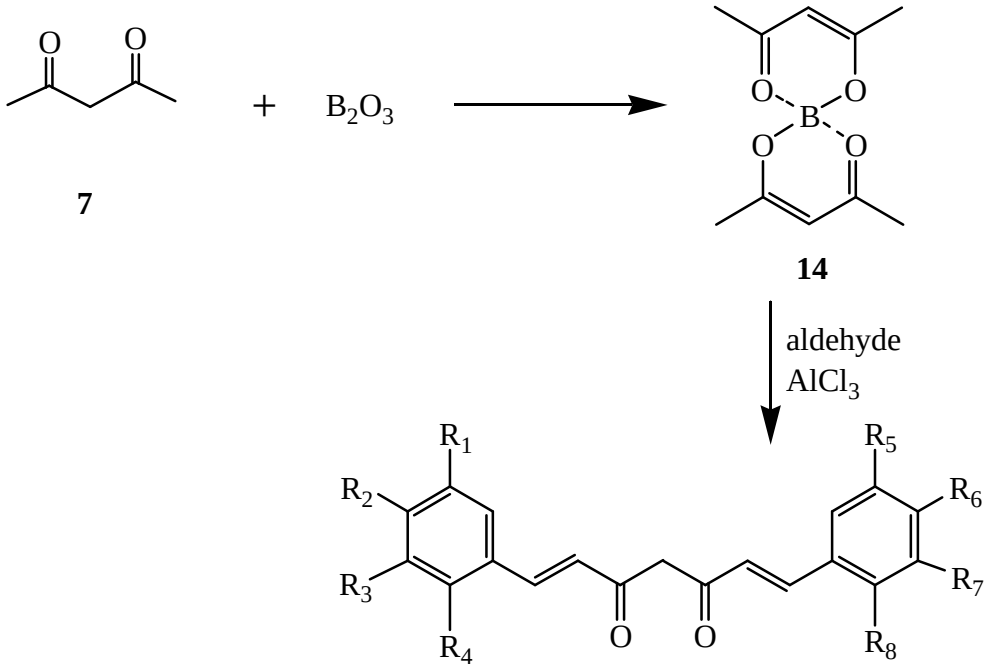

Scheme 8

3. Chemical properties

Curcumin exists in equilibrium between the diketo and keto-enol forms; the keto-enol forms is strongly favored by intramolecular H-bonding, [26] **(Fig. 1)**.

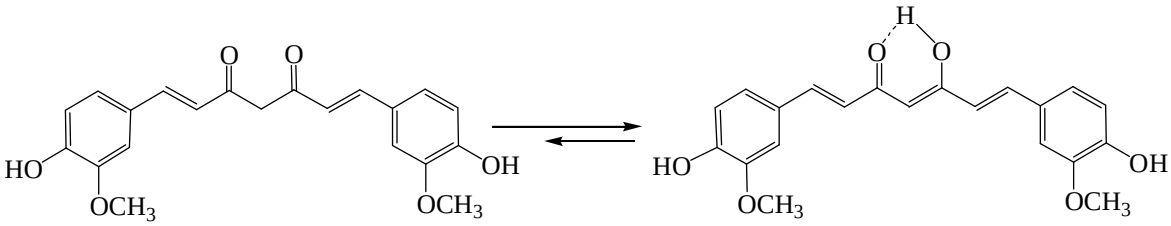

Curcumin

Fig 1. Curcumin exists in solution as an equilibrium mixture of the symmetrical dienone and the keto-enol tautomer stabilized by intra molecular H-bonding.

Curcumin **(1)** and other curcuminoids are practically insoluble in water, neutral and medium acidic pH, while soluble in both polar and non polar organic solvents. These compounds are, however, more soluble in alkaline solvents and in extremely acidic solvents, presumably due to the ionization of the phenolic or enolic groups and/or due to their dissociation forms.

There are two kinds of acidic hydrogens in curcumin **(1)**. One is a phenolic hydrogen, the other is an active methylene hydrogen of *β*-diketones. The pk_a values for the dissociation of these acidic protons in curcumin were reported to be 7.80, 8.5 and 9.0, respectively.[27]

3.1. <u>Hydrazinocurcumin (HC) formation</u>

The general procedures for the synthesis of derivatives are shown in **scheme 1** and **2**. Curcumin (**1,** R_1=R_2= OCH_3) and its natural analogues including demethoxycurcumin (**1a,** R_1= OCH_3; R_2= H or vice versa) and bis-demethoxycurcumin (**1b,** R_1= H; R_2= H) were involved in the reaction. Diketone moieties of each curcumin analogue were replaced with

hydrazine derivatives in the presence of acetic acid. One **(1)** with hydraziniumdihydrochloride and hydrazinobenzzoic acid gave compounds **(17)** to **(18)**. Each compound was purified with preparative TLC and HPLC, and was assayed for antiangiogenic activity.[28]

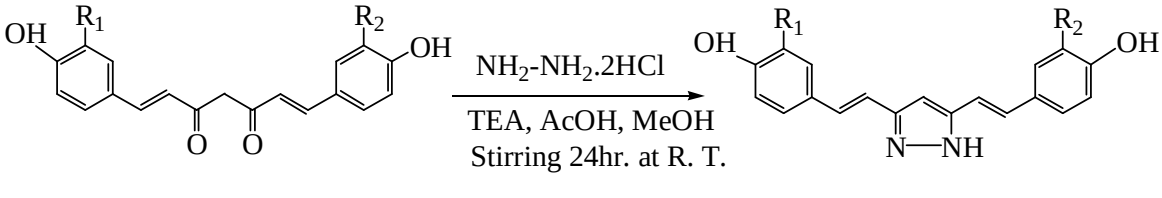

1 **17**

Scheme 9

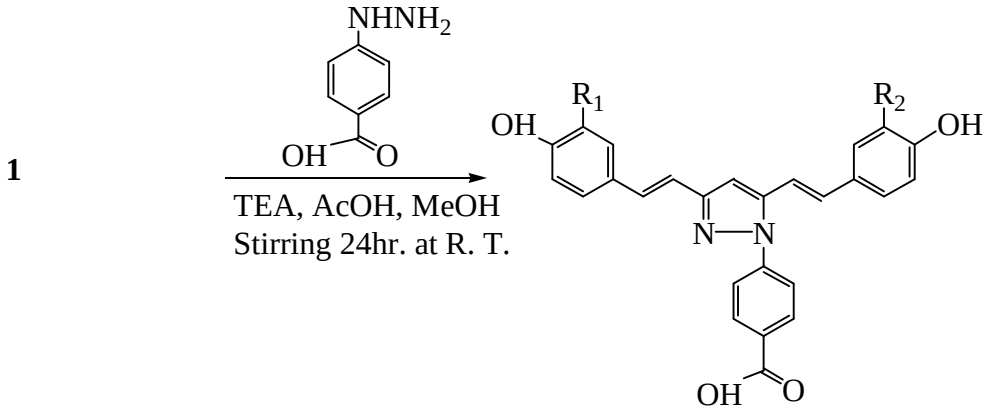

17, 18; **a**, R_1= R_2= OCH_3
b, R_1= OCH_3, R_2= H
c, R_1= R_2= H

Scheme 10

It has been reported also that, pyrazole derivatives **(17a-c)** were prepared by heating **(1-1b)** overnight with histidine hydrazide, acetic acid and *p*-TsOH.[29] The prepared pyrazole derivatives were evaluated as cytotoxic agents.

In a similar way, the pyrazole analogues **(17a-c)** were prepared by treating the CH_2Cl_2 extract of curcumin **(1-1b)** with hydrazine hydrate in

acetic acid. The reaction mixture was stirred for 7h at room temperature. The pyrazoles **(17a-c)** were synthesized for biological evaluation and molecular docking of curcumin analogues as antioxidant, cyclooxygenase inhibitory and anti-inflammatory agents.[30]

3.2. isoxazole analogue

The isoxazole analogue **(19a,b)** were prepared by treating the CH_2Cl_2 extract with hydroxylamine hydrochloride in acetic acid at 85°C for 6hr.[30]

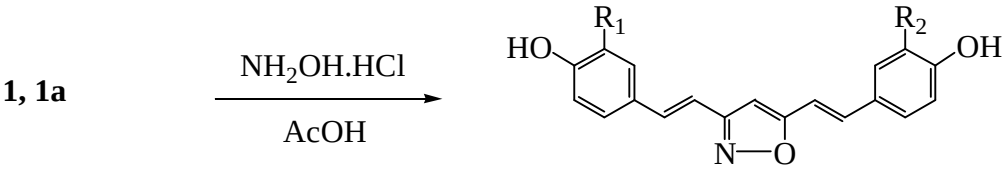

19 **a**, $R_1 = R_2 = OCH_3$

b, $R_1 = OCH_3$; $R_2 = H$

Scheme 11

3.3. Acylation and related compounds

It was reported that,[29] the reaction of anhydrous acetic anhydride with curcumin **(1)** in anhydrous pyridine with stirring at room temperature overnight was used as a route for the synthesis of the acyl derivative**(20)**.

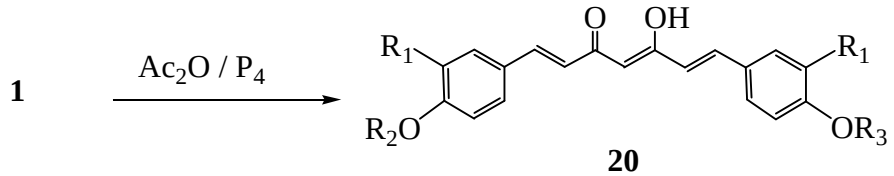

20

R_1	R_2	R_3
OCH_3	Ac	Ac

Scheme 12

Moreover, the di-*O*-acetyl derivative **(20)** was prepared by the acylation of both the phenolic functions of curcumin with acetic anhydride.[31] Similarly, the derivatives of curcumin viz, 4,4'-di-*O*-(glycinoyl)curcumin **(21)**, 4,4'-di-*O*-(D-alaninoyl)curcumin **(22)**, 4,4'-di-*O*-(piperoyl)curcumin (23) and curcumin-4,4'-di-*O*-*β*-D-glucopyranoside **(27)** were also prepared and tested for their antibacterial activity.[31,32]

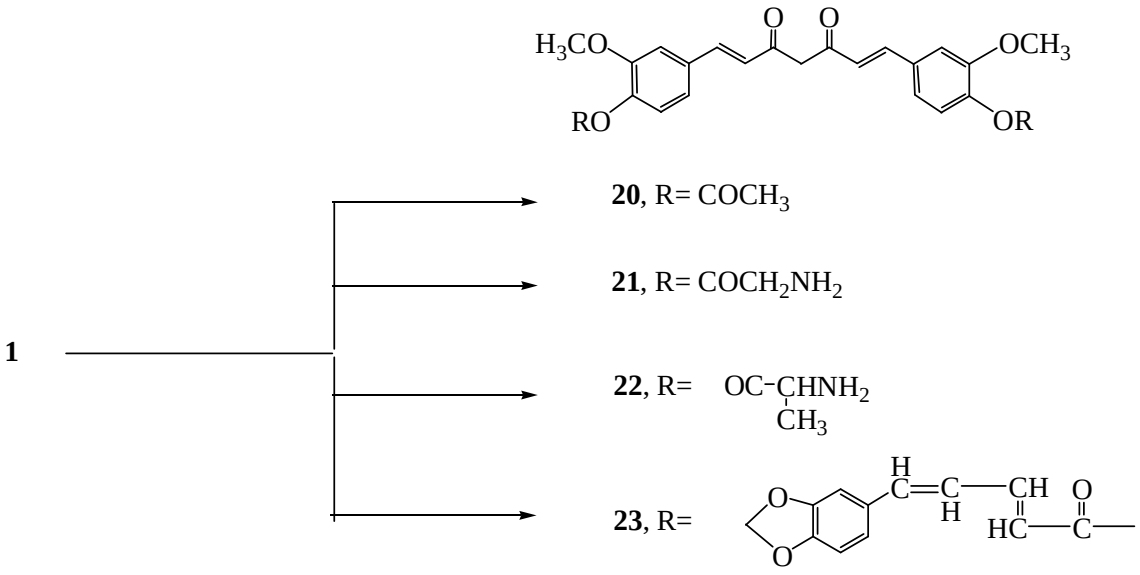

Scheme 13

Compound **(24)** was prepared according to the following **scheme 14**.

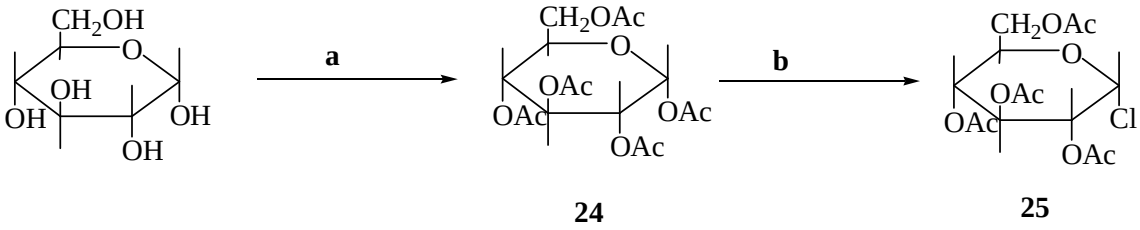

24 **25**

Synthesis of D-glucose-penta acetate **(24)** and 1-*α*-chloro-2,3,4,6-tetraacetyl-D-glucose **(25)**.

a) Dry pyridine/acetic anhydride / 0^{o}C, DMAP

b) Dry dichloroethane/dry HCl/ 0^{o}C, stirred at 0^{o}C 2.5h

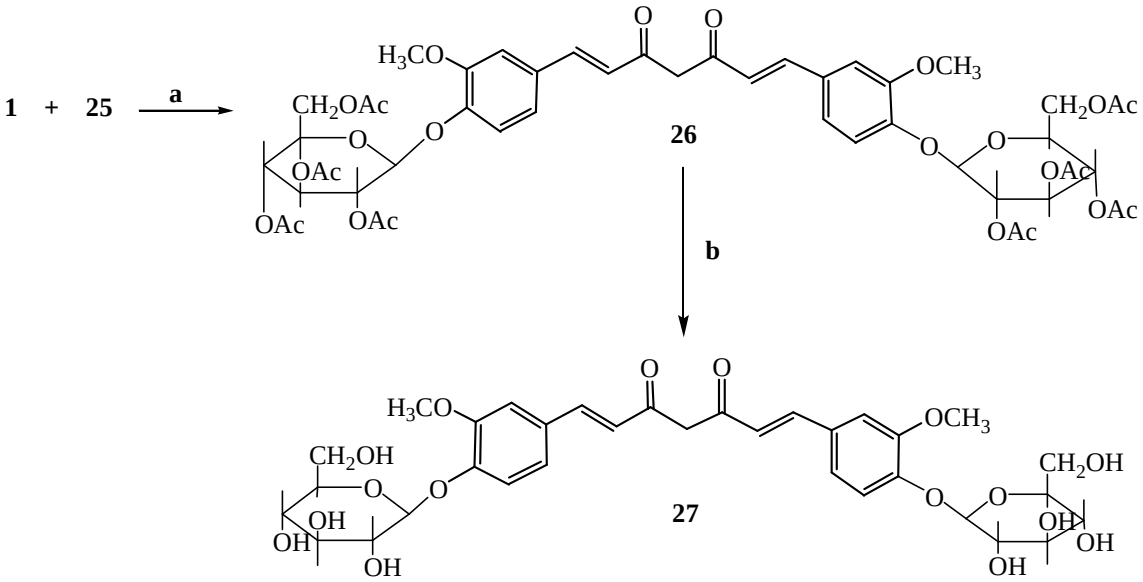

Synthesis of curcumin-4,4'-di-β-D-glucopyranoside **(27)**: a) **(26)**/pyridine, b) NH_3-MeOH (1:1 v/v) 2h at R.T.

Scheme 14

Also, 1,7-bis-4,4'-[(*O*-cystinoyl)-3-methoxyphenyl-]-1,6-heptadiene-3,5-dione **(28)** was prepared by reaction of **(1)** with fmoc-protected cystine in THF in presence of dicyclohexyl carbodiimide (DCC).[32]

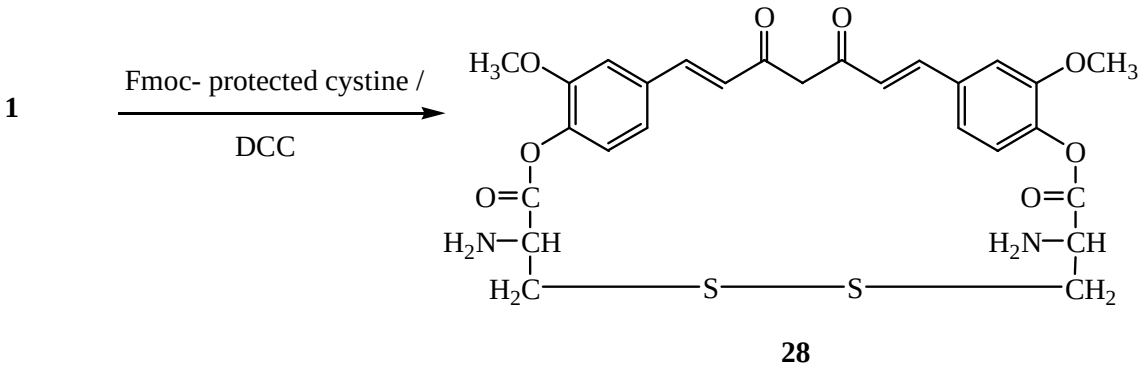

3.4. Alkylation

Refluxing of curcumin **(1)** in dry acetone with methyl iodide for 48h with stirring over anhydrous K_2CO_3 afforded methylcurcumin,[13] **(29)**. Hydrogenation of **(29)** in ethyl acetate at room temperature and 45 psi over 10% Pd/C catalyst yielded compound **(30)**.

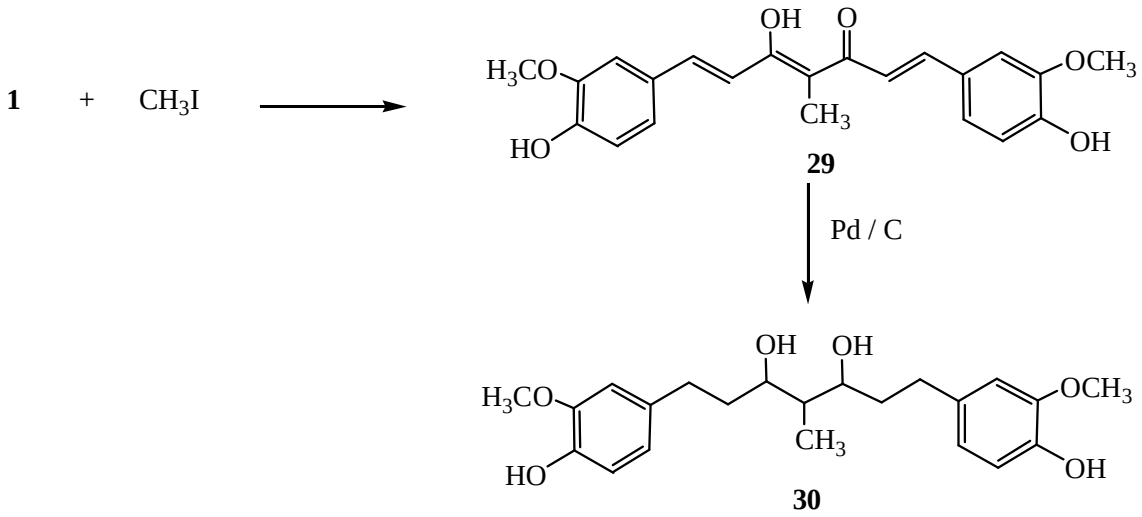

Scheme 15

Compounds **(31-35)**,[33,34] contain a 7-carbon spacer. These compounds were prepared according to the following **Scheme 16**.

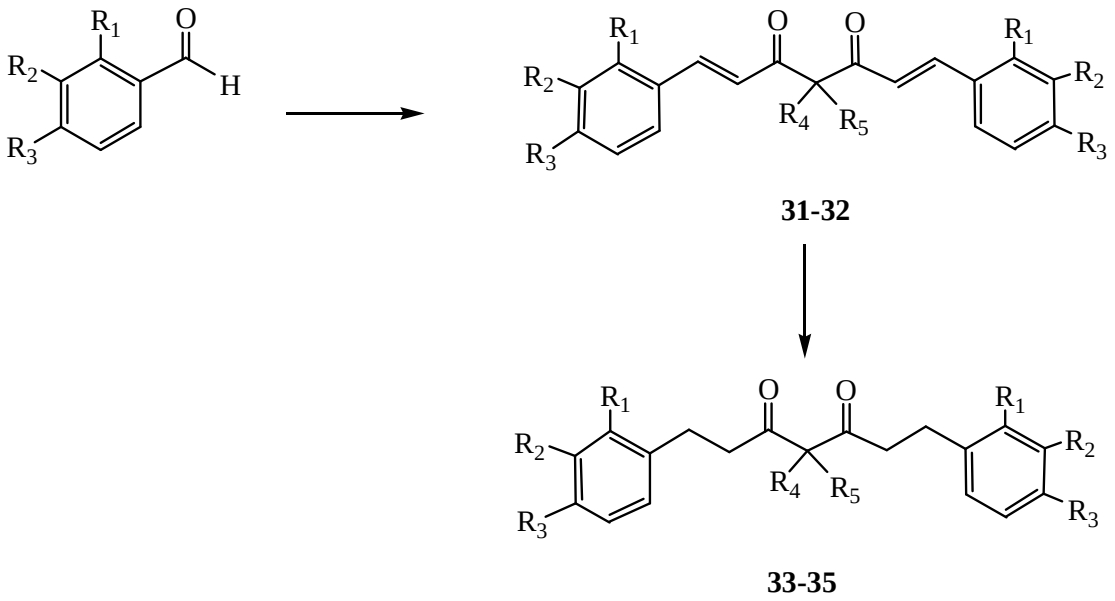

31, R_1= H; R_2= OCH_3; R_3= OH; R_4= Bn; R_5= H

32, R_1= H; R_2= OCH_3; R_3= OH; R_4= CH_3; R_5= H

33, R_1= H; R_2= OCH_3; R_3= OH; R_4= CH_3; R_5= H

34, R_1= H; R_2= H; R_3= H; R_4= Bn; R_5= Bn

35, R_1= H; R_2= H; R_3= H; R_4= CH_3; R_5= H

Scheme 16

Compounds **(31)** and **(32)** were prepared by reaction of 3-benzyl-2,4-pentandione or 3-methyl-2,4-pentanedione with 4-hydroxy-3-methoxybenzaldehyde in an aldol-type reaction following the procedure described by Papon.[11] As expected, in the proton NMR of compounds **(31)** and **(32)** the enol form predominates, whereas the carbon spectra exhibit both the keto- and enol forms.[20]

Compounds **(33-35)** contain two aryl rings separated by a saturated seven carbon spacer having two carbonyls. Compounds **(33-35)** were prepared by reduction of the corresponding unsaturated derivatives using a procedure described by venkateswarlu.[25]

Since the difference of acidity between the two kinds of hydrogens in curcumin is not large enough, as mentioned before, the alkylation or acylation reaction with alkyl halides or acyl halides yields several products such as mono-*O*-substituted **(36)**, di-*O*-substituted **(37, 39, 41, 42)** and tri-substituted (mono-4-C and di-O) compounds **(38, 40, 43)**.[35]

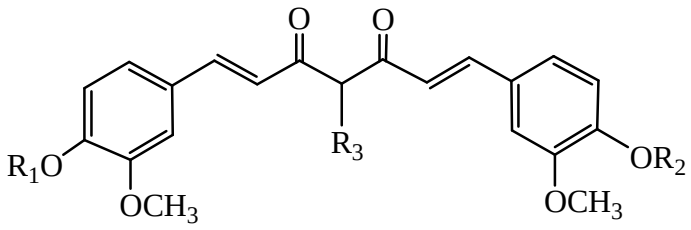

1a, $R_1= R_2= R_3= H$ **36**, $R_1= CH_3$; $R_2= R_3= H$

37, $R_1= R_2= CH_3$; $R_3= H$ **38**, $R_1= R_2= R_3= CH_3$

39, $R_1= R_2= C_6H_5CH_2$; $R_3= H$ **40**, $R_1= R_2= R_3= C_6H_5CH_2$

41, $R_1= R_2= CH_3CO$; $R_3= H$ **42**, $R_1= R_2= C_6H_5CO$; $R_3= H$

43, $R_1= R_2= R_3= C_6H_5CO$

Scheme 17

In order to increase the yield and stability of phenoxide ion and/or enolate anion during the reaction, a catalytic amount of $NaHSO_4$ and $(n\text{-}Bu)_4N^+I^-$ were added along base. It seems that metal halide or metal sulfate salt was formed to accelerate the anion formation. At the early stage of the reaction, the mono-substituted products were detected by TLC, which could not be isolated. In fact the reaction proceeded to yield the di-substituted one. Where excess methyl iodide was used and the reaction was carefully controlled by acidification of reaction mixture, mono-*O*-methylated product **(36)** could be obtained. Tri-substituted products were obtained when the reaction mixture were refluxed for sufficiently long time. Tetra-substituted products was not formed because the basicity of the base was not strong enough to make the enolate anion.[35]

3.5. Hydrogenation

Starting from curcumin **(1)** various kinds of reductive state products **(44-46)** have been described previously in the literature.[9] Further improvement with different conditions of Pt/C catalyzed hydrogenations was attempted **(Scheme 18)** providing the optimum yield of hexahydrocurcumin (**46**, 91.8%) under higher pressure and longer reaction time. Although **(45)** and **(46)** could also be obtained from **(44)** by $NaBH_4$ reduction, the yield were low. Structure **(45)**, possessing an asymmetrical skeleton, has more potential for further structural modification. Thus, direct reductive amination of **(45)** with propylamine yielded **(47)**, though the yields (16%) were not satisfactory. This could be due to intramolecular hydrogen bonding between 3-carbonyl and 5-hydroxy in **(45)**, reducing the possibility of Schiff base formation.[36] Also, it has been reported the synthesis of diarylheptylamine analogs **(48)**.

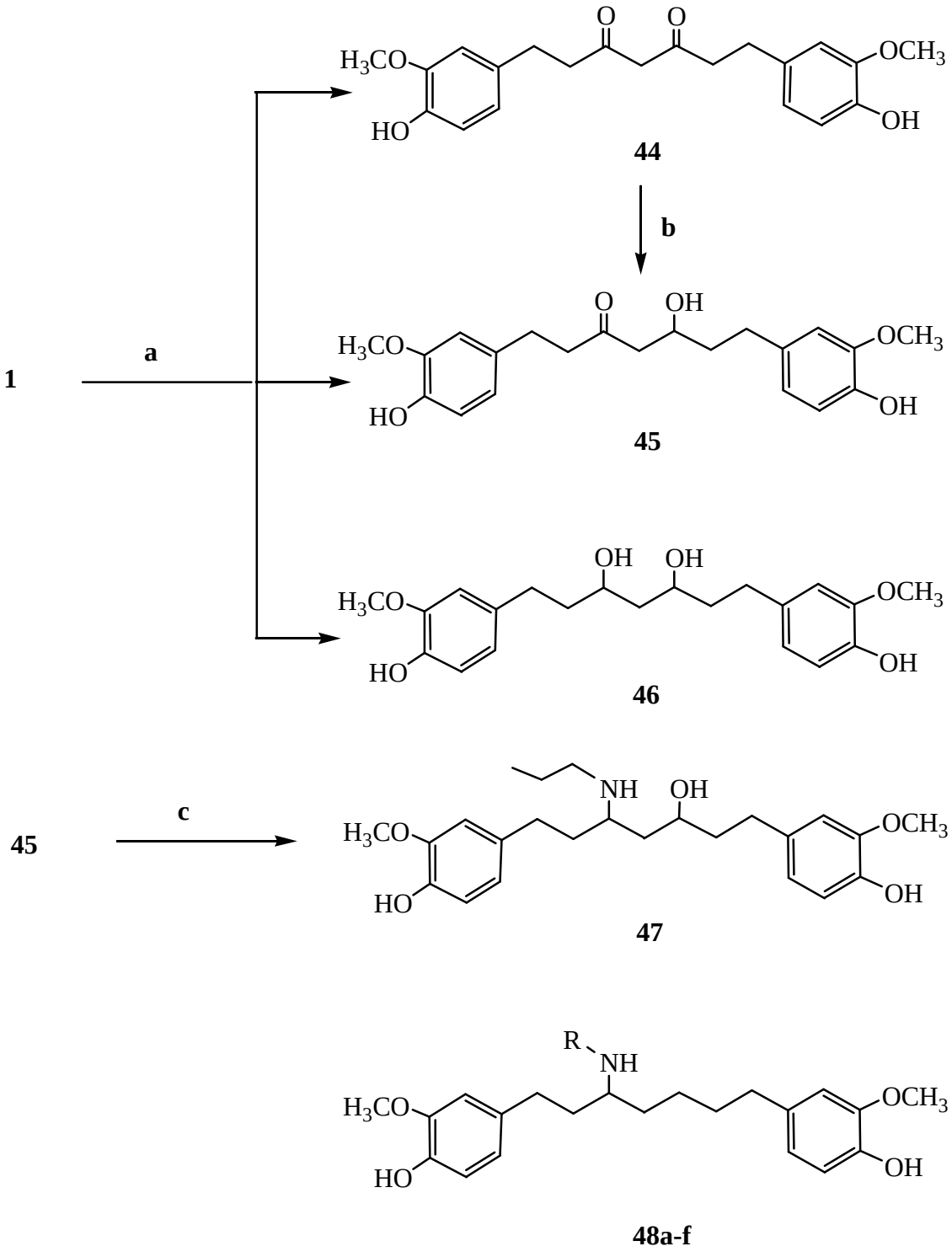

Scheme 18

Reagents and conditions: a) Pt/C, H_2, MeOH, rt;

b) $NaBH_4$, MeOH, rt, 6hr (**45**, 7%), (**5**, 19%);

c) H^+, propylamine, $NaBH_3CN$, MeOH, rt, 4days (16%).

3.6. Metal complex

Curcumin acts as an antioxidant by scavenging free radicals such as alkoxyl/phenoxyls,[37] peroxyl, hydroxyl,[38] and nitrogen dioxide radicals.[39] However, a recent study has demonstrated that curcumin is not an effective scavenger for suberoxide radical $(O^{\cdot}_2)^-$ and a large concentration of curcumin is needed to trap this radical.[40] To improve the efficacy for scavenging $(O^{\cdot}_2)^-$, manganese complex of curcumin and diacetylcurcumin (Cp-Mn**(49)** and DiAcCp-Mn **(50)**) were synthesized,[41] and their stability against hydrolysis was evaluated in buffer of various pH and in human blood serum.[42]

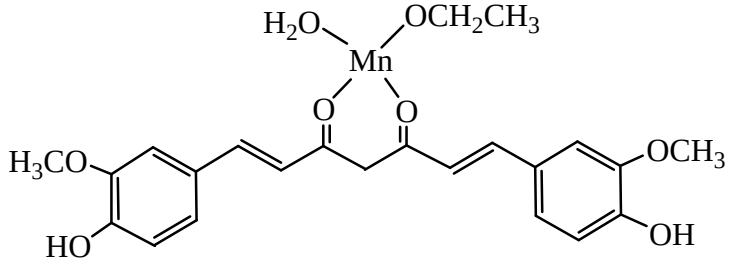

Cp-Mn
49

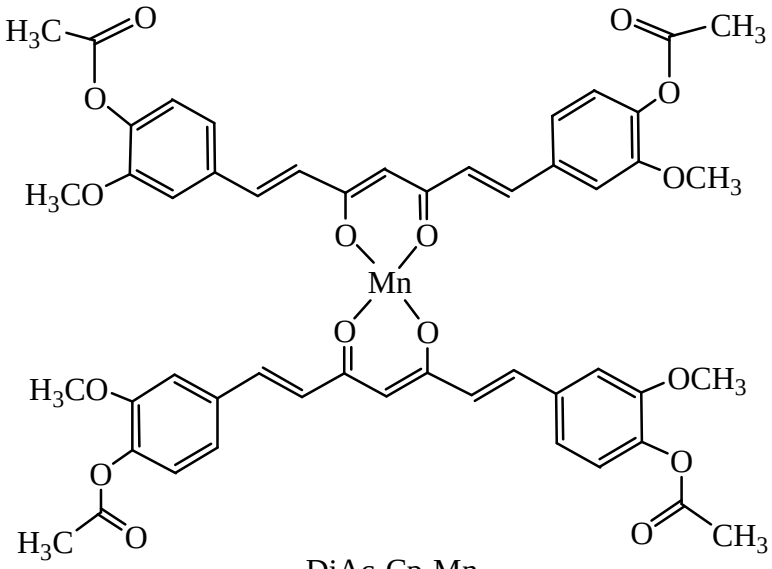

DiAc-Cp-Mn
50

Moreover, a mononuclear (1:1) copper complex of curcumin was synthesized and examined for its superoxide dismutase (SOD) activity.[43] The complex was characterized by elemental analysis, IR, NMR, UV-VIS, EPR, mass spectroscopic methods and TG-DTA, from which it was found that a copper atom is coordinated through the keto-enol group of curcumin a long with one acetate group and water molecule.

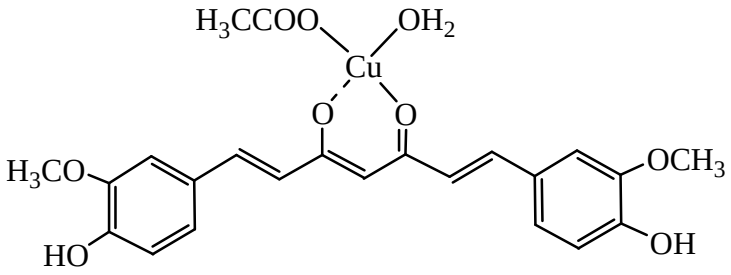

51

3.7. Spectral and Photophysical Behaviors

The absorption maximum of curcumin **(1)**, mono- and di-substituted curcuinoids is red-shifted by 50~70 nm in contrast to those of tri-substituted curcuminoids. The nature of solvent effects the absorption spectra of curcumin and curcuminoids only slightly, producing a small red-shift (ca. 0~20) after going from n-hexane to methanol.[35] Chignell *et. al.* reported that curcumin fluoresced strongly in toluene.[44] They also showed that the fluorescence intensity as well as the position of the most intense band of curcumin was very sensitive to the nature of the solvent, unlike its absorption maximum. A large red-shift in the fluorescence maximum was observed in curcumin and most of curcuminoids after going from n-hexane to methanol ($\Delta\lambda$= 77 nm), which indicates that the exited singlet state must be very polar.

4. Biological activity of turmeric and its compounds

Turmeric powder, curcumin and its derivatives and many other extracts from the rhizomes were found to be bioactive. The structures of some of these compounds.[4] are presented in Figure **1**.

Curcumin increases mucin secretion in rabbits.[45] Curcumin, the ethanol extract of the rhizomes, sodium curcuminate, [feruloyl-(4-hydroxycinnamoyl)- methane] (FHM) and [bis-(4-hydroxycinnamoyl)-methane] (BHM) and their derivatives, have high antiinflammatory activity against carrageenin-induced rat paw oedema.[46,47] Curcumin is also effective in formalin induced arthritis.[46] Curcumin reduces intestinal gas formation,[48] and carbon tetrachloride and D-galactosamine induced glutamate oxaloacetate transaminase and glutamate pyruvate transaminase levels.[49,50] It also increases bile secretion in anaesthetized dogs,[51] and rats,[52] and elevates the activity of pancreatic lipase, amylase, trypsin and chymotrypsin. [53]

Curcumin protects isoproterenol-induced myocardial infarction in rats.[54] Curcumin, FHM and BHM also have anticoagulant activity.[55,56] Curcumin and an ether extract of *C. longa* have hypolipemic action in rats,[57] and lower cholesterol, fatty acids and triglycerides in alcohol induced toxicity.[58] Curcumin is also reported to have antibacterial,[48] antiamoebic,[59] and anti HIV,[60] activities. Curcumin also shows antioxidant activity.[61-64] It also shows antitumour,[65-67] and anticarcinogenic,[68-71] activities. The volatile oil of *C. longa* shows anti-inflammatory,[72] antibacterial,[73,74] and antifungal,[74] activities. Fifty per cent ethanolic extract of *C. longa* shows hypolipemic action,[75] in rats. Ethanolic extract also possesses antitumour activity.[76] Alcoholic extract and sodium curcuminate can also offer antibacterial activity.[48,51] The crude ether and chloroform extracts of *C. longa* stem are also reported to have antifungal effects.[77]

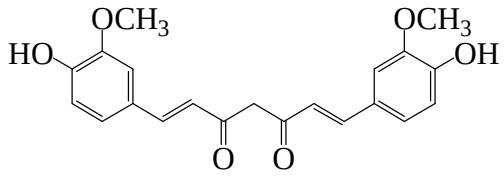

curcumin-I

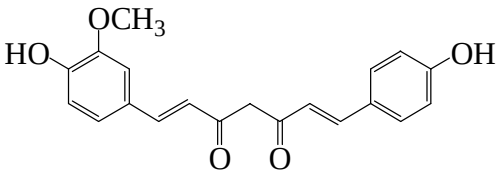

curcumin-II

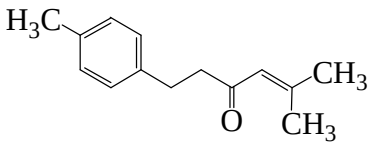

Ar- turmerone

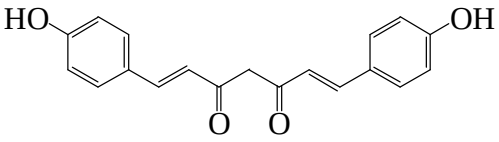

curcumin-III

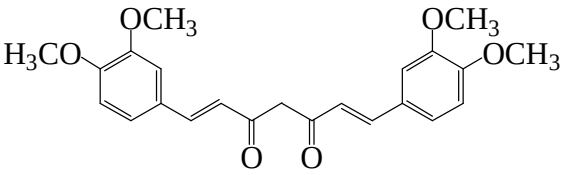

Methylcurcumin

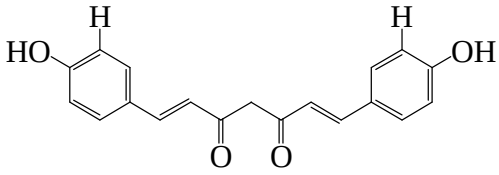

Bis-demethoxycurcumin

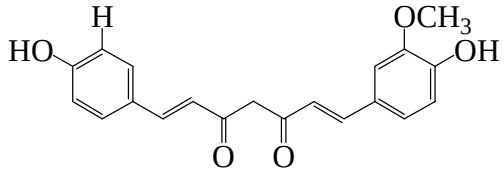

Demethoxycurcumin

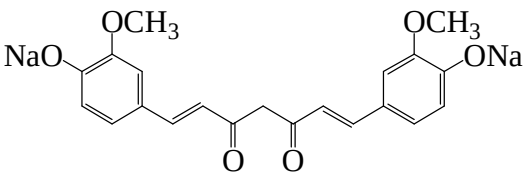

Sodiumcurcuminate

Figure 1. structure of natural curcuminoids

B) Corrosion Theory and Corrosion Protection

1. Historical overview on corrosion

Corrosion of metals has been reported as early as 1800's.[78] Significant contribution by Evans,[79] Uhling, and Pourbaix,[80] too laid a solid foundation for understanding corrosion process, research, and development. The most important electrodic process of vast practical significance is that resulting from metal dissolution in a solution or in the formation of a film of conducting moisture adhering to a metal surface. The process is termed "corrosion". The electrodic process determines the significance of corrosion. Corrosion is a reversion or a partial reversion from the meta stable condition of the metal to a stable condition of the mineral accompanied by a reduction in the free energy of the system. The most common material's corrosion is rusting of iron and the tarnishing of silver, copper etc. The rate of the metal dissolution is governed by materials characteristics and the environment.

2- Corrosion and prevention

The corrosion of metals in aqueous solutions is an electrochemical process. The mechanism of corrosion was described earlier by Wollaston,[81] and Whitney,[82] they gave the most acceptable electrochemical theory of corrosion. The acid and colloidal theories were proposed by Calvert and Walker,[83] Cederholm, Bent,[84] and Friend.[85] The chemical attack theory was proposed by Bengough, and Stuart.[86] Subsequently Reddie and Linderman ,[87] proposed the biological theory. All the above theories have been proved to be a part of the electrochemical theory.

Wollaston,[81] proposed an electrochemical theory of corrosion which was initially developed by De La Rive,[88] and was confirmed by Ericson Aure'n and Palmer.[89] Tenard,[90] confirmed that iron does not decompose in

seawater when both of them are perfectly pure. But once oxidation started, it can continue by the action of water alone.

De La Rive,[91] noticed the striking differences in the behavior of the action of sulphoric acid on pure zinc and impure metal. He concluded that impure zinc was vigorously attacked due to galvanic couple formed between zinc and its impurities. Later he extended his theory for the atmospheric corrosion of metals and concluded that corrosion was electrochemical in nature, where, Becquerel,[92] said that a cell could be produced by a single electrolyte of two different concentrations. Mellet ,[93] utilized this to explain the localized corrosion of iron casting in a tidal wave system. Adie,[94] reported that cells were formed due to the difference in oxygen concentration. Evans,[95] succeeded in demonstrating these differential aeration cells.

Whitney,[82] worked on the problem of corrosion of steel pipes in water and concluded that the process was electrochemical in nature since iron passed into the solution as ferrous ions, and corrosion rate was shown to be governed by the electromotive force of the cell set upon the iron surface. Evans and Hoar,[96] gave evidence for the electrochemical setup on steel vertically immersed in steel plate in potassium chloride solution by measuring the current passing between the lower and upper portions of the steel plate. They also gave the potential vs. current curves for both the anodic and cathodic regions set upon the steel that is now known commonly as Evans diagram. In the subsequent survey we will concentrate on the electrochemical corrosion of copper and its alloys.

3- Methods used for studying the rate of corrosion

3.1- Non-electrochemical methods

In these methods, the corrosion rate is evaluated by measuring i-the change in the weight of coupon after exposing the metal specimen of known area to the particular environment for a specific period,[97] ii-solution analysis,[98] and Gas-volumetric method In this method,[99] in which a definite correlation between the cathodic reaction rate and the anodic dissolution rate can be established.

3.2- Electrochemical methods

These methods include: i- electrical resistance method,[100] and ii- tafel extrapolation method,[101] this method was described as Tafel plot method or Evan's diagram method or logarithmic polarization method. Actually the measurement of corrosion rate of the system involves the measurement of potential of the electrode for various applied current densities. A plot of E vs log i_{corr} gives a figure known as polarization diagram. The intercept of anodic and cathodic Tafel lines provides the corrosion current and Tafel slopes give β_a, and β_c. In actual practice, polarization curves are obtained from galvanostatic / potentiostatic or potentiodynamic methods.

4- Dezincification

Dezincification selectively removes zinc from the alloy, leaving behind a porous, copper-rich structure that has little mechanical strength. Dezincification generally occurs in copper-zinc alloys containing more than 15% zinc because of zinc is a highly reactive metal, this reactivity stems from the fact that zinc has a very weak atomic bond relative to other metals. Simply, zinc atoms are easily given up to solutions with certain aggressive characteristics. During dezincification, the more active zinc is

selectively removed from the brass, leaving behind a weak deposit of the porous, more noble copper-rich metal.

Brasses are basically Cu-Zn alloys and are the most widely used groups of copper alloys. The resistance of brasses to corrosion by aqueous solution does not change markedly as long as the zinc content does not exceed about 15%. Above 15% zinc, dezincification may occur. Quiescent or slowly moving saline solution, brackish waters, and mildly acidic solution are environments that often lead to the dezincification of unmodified brasses. Susceptibility to stress-corrosion cracking (SCC) is significantly affected by zinc content. Alloys that contains more zinc are non susceptible to SCC. Elements such as Pb, Te, Be, Cr, P and Mn have little or no effect on the corrosion resistance of copper and binary copper-zinc alloys.

Brass is a material commonly used in the manufacture of very different products like electrodes for batteries, decorative or functional objects and parts of engines and machinery, as well as pipelines and tubes, and it is easily cut and polished. The final use of a Cu/Zn alloy is determined by its chemical and phase composition because these greatly influence quality and properties of the alloy. The chemical composition of the alloy is easy to determine but the phase identification requires the use of techniques that are not so easy to handle or interpret, such as X-ray diffraction or electron microscopy. Moreover, these techniques are expensive and the instruments are not portable. This implies the transport of the sample to the laboratory for analysis and, in many cases, it has to be cut or handled to cope with the sample requirements of the instrumentation. This is sometimes impossible, especially when the sample is an art object, a piece of a pipeline or a part of working machinery. Electroanalytical techniques are powerful tools to study brass since they offer valuable

information about the phase and chemical composition.[102] Such techniques have also proved to be useful to study the evolution of brass in the environment,[103] as well as in different media to understand the degeneration process and to prevent oxidation of the alloy better.[104-106]

5- Literature Survey on Corrosion of *α*-Brass

Corrosion inhibition efficiencies of triazole derivatives for 70–30 brass in water containing 3% NaCl have been evaluated by means of weight loss, electrochemical polarisation, and impedance techniques.[107] The triazole derivatives, namely aminomethyl mercaptotriazole (AMMT), aminoethyl mercaptotriazole (AEMT), and aminopropyl mercaptotriazole (APMT), gave inhibition efficiencies in the order APMT (94·5%) > AEMT (93·6%) > AMMT (91·5%). Nyquist plots showed Warburg impedancœ, i.e. the reaction was under diffusion control. T he inhibition efficiencies of the triazoles did not drop under dynamic flow conditions. Solution analysis showed selective dissolution of zinc compared with copper. The lowest concentration of zinc, achieved in the tests with the optimum inhibitor addition, was 0.35 mg L^{-1}.

The efficiency of two newly developed organic compounds of the triazoles type namely: bis[4-amin-5-hydroxy-1,2,4-triazol-3-yl]-methane "compound D_1" and bis[4-amino-5-hydroxy-1,2,4-triazol-3-yl]-butane "compound D_2" as corrosion inhibitors for copper in 4.0M HNO_3 solutions at 25^{o}C was investigated using both weight loss and galvanostatic polarization techniques.[108] The results showed that the predominant action of the inhibitors was cathodic. The two inhibitors proved to be effective (>99%) with long term effectiveness. Galvanostatic polarization measurements confirm weight loss measurements.

The homologous series of aromatic secondary amines with various substituents have been investigated.[109] The results of the electrochemical and gravimetric measurements on copper in hydrochloric and sulfuric acid have shown that the nonsubstituted secondary amine (N-(2-furfuryl)-*p*-toluidine) has the least-effective inhibiting properties. The introduction of substituents (-Cl, -Br, $-NO_2$, $-CH_3$) in the 5-position of N-(2-furfuryl-*p*-toluidine) increased the degree of copper protection in acid media. The pyrophosphate electrolyte has been used for brass deposition as a replacement for cyanide electrolytes.[110] However, there is considerable confusion about the current efficiency of brass deposition from this electrolyte. This study uses a rotating disc electrode (RDE), a rotating cylinder electrode (RCE) and a quartz crystal microbalance (QCM) to systematically determine the current efficiency of copper, zinc, and brass deposition from a pyrophosphate electrolyte. The current efficiency for copper, zinc as well as brass was below 100%. Simultaneous measurement of current and frequency at a QCM showed that pyrophosphate is adsorbed at the electrode surface during copper reduction.

Corrosion inhibition efficiencies of triazole derivatives for 70–30 brass in water containing 3% NaCl have been evaluated by weight loss, electrochemical polarisation, and impedance techniques.[111] The triazole derivatives, namely aminomethyl mercaptotriazole (AMMT), aminoethyl mercaptotriazole (AEMT), and aminopropyl mercaptotriazole (APMT), gave inhibition efficiencies in the order APMT (94·5%) > AEMT (93·6%) > AMMT (91·5%). The inhibition efficiencies of the triazoles did not drop under dynamic flow conditions. Solution analysis showed selective dissolution of zinc compared with copper. The kinetics of the electropolymerization of 2-mercaptobenzimidazole (2-MBI) on a brass substrate in alkaline solution containing methanol was investigated using

cyclic polarization, chronoamperometry and electrochemical impedance techniques.[112] The polymeric film was prepared by successive cycles of potential of a Cu–Zn electrode between 0.2 and 2.4 V. During the second cycle, the oxidation peak of the monomer disappears indicating the formation of the insulating film. The protective effect of the film formed on brass has been studied in a 3% NaCl solution.

Acoustic emission (AE) associated with electrochemical measurements (electrochemical impedance spectroscopy and polarization curves) are used to study the selective corrosion of *α*,*β*-brass in an ammonia buffer solution.[113] AE reveals, in this work, three different populations of events during the corrosion of this alloy. The corrosion process was found to proceed via oxygen reduction following a diffusion-controlled mechanism and selective dissolution of *α*,*β*-brass was controlled by the zinc atoms diffusion through oxide film. The diffusion coefficient obtained for zinc in *α*,*β*-brass following Cottrell law is of the order of 9.28 X 10^{-12} cm^2/s. The selective dissolution of brass was studied using potentiodynamic polarization, coloumetric analysis and electrochemical impedance spectroscopy (EIS).[114] Using coloumetric analysis, the partial currents i_{Zn} and i_{Cu} were measured under various potentials and chloride concentrations. Chloride ions promote the dissolution of Zn and Cu and hence increase the rate of dissolution of the alloy. At active potentials, zinc dissolves preferentially leaving the alloy surface enriched in copper. Under this condition, the polarization resistance of the interface and its double layer capacity increase with the time and extent of dissolution of the alloy. As the chloride concentration increases and/or the potential shifts in the noble direction, the rate of copper dissolution increases so that simultaneous dissolution of both components is observed. This increase in the rate of copper dissolution is enhanced by the higher stability of the copper chloride complex ($CuCl^{2-}$) compared to zinc chloride ($ZnCl_2$). New

brass and copper alloys offer high strength as well as excellent retention of strength at elevated operating temperatures.[115] They can withstand high-temperature brazing processes without a substantial loss in strength. A brazing center has been established to demonstrate this new brazing process and evaluate the technology through prototype building.

Cyclic voltammetry has been used to investigate the behaviour of copper surfaces in aqueous solutions of sodium salicylate.[116] The observed copper anodic passivation dependence on the presence of salicylate ion in solution is explained. The analysis of the experimental data supports the formation of a complex passivating film formed by a Cu_2O inner layer and a mixed cupric oxide/cupric salicylate outer layer; this film provides a partial passivation of the copper surface and can be completely removed upon excursion to negative potentials values. The composition of the passivating layer depends on the electrolyte nature, i.e. sodium salicylate ion and solution pH, and on the potential programme the copper electrode is subjected to.

The effect of novel corrosion inhibitors, benzotriazole derivatives namely *N*,*N*-dibenzotriazol-1-ylmethylamine (DBMA), and 2-hydroxy ethyl benzotriazole (HEBTA) on the corrosion and dezincification of a 65/35 brass in 3% NaCl has been investigated by weight-loss, potentiodynamic polarization, electrochemical impedance and solution analysis techniques.[117] Polarization studies clearly indicated that the benzotriazole derivatives behave as anodic inhibitors for brass in chloride solutions. They decrease the anodic reaction rate more strongly than the cathodic reaction rate and render the open circuit potential of brass more positive in NaCl solutions. Solution analysis revealed the decrease in dissolution of both copper and zinc in the presence of these inhibitors.

The study of Boc–Phe–Met–OCH3 as corrosion inhibitor for 60Cu–40Zn in nitric acid solution was performed through weight loss and electrochemical polarisation measurements.[118] The corrosion rate is highly reduced in the inhibited nitric acid. The inhibition efficiency E (%) reached a maximum value of 100% for Boc–Phe–Met–OCH3. Polarisation measurements indicated that Boc–Phe–Met–OCH3 acted as cathodic inhibitors without changing the mechanism of the hydrogen evolution reaction. The results showed that the inhibition occurred via chemisorption of the inhibitor molecules on the corroding metal following Frumkin's isotherm. The electrochemical behaviour of brass was studied in artificial seawater with two organic inhibitors namely *N*,*N*-dibenzotriazol-1-ylmethylaminomethane (DBMM) and 3-hydroxypropyl benzotriazole (HPBT) using potentiodynamic polarization, electrochemical impedance spectroscopy (EIS), cyclic voltammetry and current transient techniques.[119] Polarization measurements showed that the organic compounds investigated are mixed type inhibitors, inhibiting the corrosion of brass by blocking the active sites of the metal surface. Changes in the impedance parameters (charge transfer resistance (Rct) and double layer capacitance (Cdl)) are related to adsorption of organic inhibitors on the metal surface, leading to the formation of a protective film, which grows with increasing exposure time.

The synthesis of poly pyrrole film was achieved on brass and copper electrodes, employing cyclic voltammetry technique, from monomer containing 0.3M oxalic acid solutions.[120] The corrosion performance of PPy coated samples were investigated in 0.1M H_2SO_4 solutions, using the electrochemical impedance spectroscopy (EIS), anodic polarization curves and open circuit potential (E_{ocp})–time curves. It was shown that PPy coating could provide important protection against the corrosion of copper and

brass. However, polymer coating gave better results with copper with respect to brass. The presence of Pseudomonas fluorescence in artificial tap water (ATW) affects the composition of the oxide layer and the susceptibility to pitting corrosion of copper and 70/30 brass.[121] The surface layer was investigated by means of a combination of electrochemical and spectroelectrochemical techniques involving cyclic voltammograms, potentiodynamic reduction curves, anodic polarisation curves, weight-loss tests and reflectance spectroscopy. Dezincification in inoculated electrolyte was revealed by microscopic observation, as well as by potentiodynamic reduction curves. Zn dissolution was also supported by spectroscopic evidence. Slow-rate voltamperometric curves were used to determine potential values characteristic of localized corrosion. In the presence of bacteria, the pitting potential moves towards more positive values for both materials but the difference between the repassivation and the pitting potential increases. Bigger and deeper pits can be seen in the presence of microorganisms.

The electrochemical behaviour of brasses with various Zn content (5.5–38 mass %) and brass (Cu–38Zn) with different Pb contents (1–3.4 mass %) in 0.6M NaCl was investigated.[122] The effects of temperature, immersion time, and concentration of chloride ions on the behaviour of the different alloys were studied. The pitting corrosion behaviour of Cu–Zn alloys and leaded–brass alloys in 0.6M NaCl solution was also investigated. Open-circuit potential measurements (OCP), polarization techniques and electrochemical impedance spectroscopy (EIS) were used. The results show that the increase in the Zn content increases the corrosion rate of the brass alloys in chloride solutions, while the increase of Pb content in Cu–38Zn–Pb decreases the corrosion rate of the alloy. Long

immersion time of the alloys in the aqueous electrolyte improves their stability due to the formation of passive film on the alloy surface.

Different electrochemical methods such as polarization, open-circuit potential measurements techniques and electrochemical impedance spectroscopy (EIS) were used to investigate the electrochemical behaviour of brass alloys with various Zn contents (5.5–38.0 mass %) and Cu–38.0Zn–Pb alloy with different Pb contents (1.0–3.4 mass %) in neutral sodium sulfate solutions.[123] The influence of working conditions, e.g., immersion time, sulfate ions concentration and temperature on the electrochemical behaviour of the different alloys was also studied. It was found that the initial corrosion rate is relatively high for alloys with the higher zinc content due to dezincification. The dezincification process initiates by selective dissolution of zinc and continues by a simultaneous dissolution of copper and zinc followed by re-deposition of copper. An increase in the lead content and immersion time in the sodium sulfate solution increases the corrosion resistance of the alloy and improves its stability.

The corrosion behaviour of brass in the presence of two organic inhibitors that belong to the benzotriazole derivatives namely *N*-[1-(benzotriazol-1-yl) methyl] aniline (BTMA) and 1-hydroxy methyl benzotriazole (HBTA) has been investigated in neutral aqueous NaCl solution.[124] Weight-loss measurements, potentiodynamic polarization and electrochemical impedance spectroscopy (EIS) were applied to analyze the effect of the organic compounds on the corrosion inhibition of brass. Polarization studies showed that these inhibitors were found to act as mixed type for brass in chloride solution. It suppresses the cathodic and anodic reactions rates and it renders the open circuit potential to more noble

directions. Solution analysis was used to calculate the dezincification factor. FTIR was used to characterize the surface film.

The electrochemical behavior of brass was studied in artificial seawater with two organic inhibitors namely *N*,*N*-dibenzotriazol-1-methylaminomethane (DBMM) and 3-hydroxypropyl benzotriazole (HPBT) using potentiodynamic polarization, electrochemical impedance spectroscopy (EIS), cyclic voltammetry and current transient techniques.[125] Changes in the impedance parameters (charge transfer resistance (Rct) and double layer capacitance (Cdl)) are related to adsorption of organic inhibitors on the metal surface, leading to the formation of a protective film, which grows with increasing exposure time. Cyclic voltammetric studies confirmed that the addition of inhibitors effectively inhibits the anodic dissolution of brass in artificial seawater.

The effect of new corrosion inhibitors namely *N*-[1-(benzotriazol-1-yl)ethyl]aniline (BTEA), and *N*,*N*-dibenzotriazol-1-ylmethylaminoethane (DBME) on the dezincification of 65–35 brass in sodium chloride solution was investigated using weight-loss measurements and electrochemical techniques such as potentiodynamic polarization and electrochemical impedance spectroscopy.[126] Results obtained revealed that these compounds were very good inhibitors and behaved better in NaCl solution. Polarization studies showed that the BTEA and DBME behave as a mixed-type of inhibitors for 65–35 brass in sodium chloride solution. They decrease the anodic reaction rate more strongly than the cathodic reaction rate and renders the open circuit potential of brass more positive in NaCl solutions.

The effect of the addition of some tetrazolic type organic compounds: 1-phenyl-5-mercapto-1,2,3,4-tetrazole (PMT), 1,2,3,4-

tetrazole (TTZ), 5-amino-1,2,3,4-tetrazole (AT) and 1-phenyl-1,2,3,4-tetrazole (PT) on the corrosion of brass in nitric acid is studied by weight loss, polarization and electrochemical impedance spectroscopy (EIS) measurements.[127] The explored methods gave almost similar results. Results obtained reveal that PMT is the best inhibitor and the inhibition efficiency (E%) follows the sequence: PMT > PT > AT > TTZ. Polarization measurements also indicated that tetrazoles acted as mixed-type inhibitors without changing the mechanism of the hydrogen evolution reaction. Partial π-charge on atoms has been calculated. Correlation between the highest occupied molecular orbital energy E_{HOMO} and inhibition efficiencies was sought. The adsorption of PMT on the brass surface followed the Langmuir isotherm. Effect of temperature is also studied in the (25–50 °C) range.

The inhibition of two terdentate ligands, 2-[(*E*)-pyridin-2-ylimino) methyl)] phenol and 2-[(pyridin-2-ylamino) methyl] phenol, abbreviated L1 and L2 respectively, on the corrosion of brass in 0.10 M NaCl solution under various conditions, has been studied by means of the potentiostatic polarization and AC impedance methods.[128] Self-assembled films of these substances were also prepared on the brass surface. These films improved significantly the protecting ability of brass surface to corrosion in 0.1 M NaCl solution. When the films were modified with benzotriazole (BTA), the quality and corrosion resistance of films improved markedly. The effect of potassium ethyl xanthate (EtX^-) on the anodic dissolution of copper in acidic sodium chloride solutions was studied using voltammetry on a rotating disc electrode (RDE) and electrochemical quartz crystal microbalance (EQCM) techniques.[129] The compound used at 5×10^{-3} M concentration acts as a strong inhibitor against copper dissolution. The inhibitory action increases with an increase in pH of the solution. The

influence of EtX^- on the spontaneous dissolution of copper was also investigated.

The influence of derivatives of 1,2,4 triazole, 3-amino 1,2,4-traizole (ATA), 3-amino 5-mercapto 1,2,4 triazole (AMT) and 3-amino 5-methylthio 1,2,4 triazole (AMTT) and ionic surfactants cetyl trimethyl ammonium bromide (CTAB) and sodium dodecyl sulphate (SDS) on the corrosion control of copper in acidic solution was investigated by gravimetric and electrochemical methods.[130] The combined effect of triazoles and surfactants was also evaluated. Electrochemical parameters like corrosion potentials corrosion current density, corrosion rates and inhibition efficiencies were determined. The results reveal the fact that of all triazoles AMTT shows best inhibition and anionic surfactant SDS protects the surface better than the cationic surfactant CTAB. The polarization data reveal that all inhibitors behave as a mixed type inhibitor. Adsorption of these inhibitors on the surface of copper is found to obey the Langmuir adsorption isotherm.

The corrosion behavior of (63Cu37Zn) brass in a solution of sodium tetraborate, at pH 10.0, with the addition of chloride ions and benzotriazole (BTA) inhibitor has been reported.[131] The application of cyclic voltammetry has led to the conclusion that the anodic current densities increase with increase in immersion time in sodium tetraborate solution as well as in solutions of sodium tetraborate containing chloride ions of various concentrations. The values of anodic current density are considerably smaller in sodium tetraborate solutions with the addition of BTA compared with those in the inhibitor-free solution. The study also analyses the electrochemical behavior of 63Cu37Zn brass after various times of alloy exposure to BTA solution, as well as its behavior in BTA solutions of various concentrations.

Corrosion inhibition of benzotriazole (BTAH) for 70/30 brass in 0.1 M NaCl has been evaluated by means of electrochemical polarization and solution analysis.[132] The anodic polarization curve displays two potential regions. In the first anodic region between −1.75 and 0.0 V (SCE), benzotriazole addition enhances ZnO film formation. Cu(I) BTA film is also formed by electron transfer in this region. In the second region between 0.0 and 1.0 V (SCE) copper oxidizes to Cu(I) oxides and Cu(II) hydroxide with the formation of CuCl film. Insoluble Cu(I) BTA film complex is also formed on these oxide/hydroxide films.